

Pathways to massive black holes and compact star clusters in pre-galactic dark matter haloes with virial temperatures $\gtrsim 10000\text{K}$

John A. Regan^{*} & Martin G. Haehnelt

¹ *Institute of Astronomy, Madingley Road, Cambridge CB3 0HA*

25 March 2021

ABSTRACT

Large dynamic range numerical simulations of atomic cooling driven collapse of gas in pre-galactic DM haloes with $T_{\text{vir}} \sim 10000\text{K}$ show that the gas loses 90% and more of its angular momentum before rotational support sets in. In a fraction of these haloes where the metallicity is low and UV radiation suppresses H_2 cooling, conditions are thus very favourable for the rapid build-up of massive black holes. Depending on the progression of metal enrichment, the continued suppression of H_2 cooling by external and internal UV radiation and the ability to trap the entropy produced by the release of gravitational energy, the gas at the centre of the halo is expected to form a supermassive star, a stellar-mass black hole accreting at super-Eddington accretion rates or a compact star-cluster undergoing collisional run-away of massive stars at its centre. In all three cases a massive black hole of initially modest mass finds itself at the center of a rapid inflow of gas with inflow rates of $\gtrsim 1 M_{\odot} \text{yr}^{-1}$. The massive black hole will thus grow quickly to a mass of 10^5 to $10^6 M_{\odot}$ until further inflow is halted either by consumption of gas by star formation or by the increasing energy and momentum feedback from the growing massive black hole. Conditions for the formation of massive seed black holes in this way are most favourable in haloes with $T_{\text{vir}} \sim 15000\text{K}$ and $V_{\text{vir}} \sim 20 \text{km sec}^{-1}$ with less massive haloes not allowing collapse of gas by atomic cooling and more massive haloes being more prone to fragmentation. This should imprint a characteristic mass on the mass spectrum of an early population of massive black hole seeds in pre-galactic haloes which will later grow into the observed population of supermassive black holes in galactic bulges.

Key words: Cosmology: theory – large-scale structure – black holes physics – methods: numerical

1 INTRODUCTION

Rees (1978) in his famous “flow chart” has mapped out many possible pathways leading to the formation of a massive black hole. The discovery of very luminous high redshift quasars by the Sloan Digital Sky Survey at redshifts greater than 6 is widely seen as an important clue in this respect. The presence of super-massive black holes (SMBHs) as massive as 3×10^9 at these early times (Haiman & Loeb 2001; Fan 2001; Fan et al. 2006) requires a rapid and efficient build-up of SMBHs, challenging models based on Eddington limited growth of stellar mass black holes (e.g. Volonteri et al. 2003; Volonteri & Rees

2005; Haiman 2006; Lodato & Natarajan 2006; Volonteri 2007). The collapse of gas in pre-galactic haloes with virial temperatures close to but above the threshold for atomic cooling driven collapse is perhaps the most promising route to the fast formation of massive black holes in the mass range of $10^4 - 10^6 M_{\odot}$ which then can act as seeds for the growth of SMBHs (e.g. Haehnelt & Rees 1993; Umemura et al. 1993; Eisenstein & Loeb 1995; Kauffmann & Haehnelt 2000; Oh & Haiman 2002; Bromm & Loeb 2003; Koushiappas et al. 2004; Begelman et al. 2006; Lodato & Natarajan 2006; Volonteri et al. 2008; Tanaka & Haiman 2008).

Early attempts to simulate the collapse of gas in such haloes numerically confirmed analytical arguments that the gas should not fragment efficiently if neither metal nor H_2 cooling are important (Bromm & Loeb 2003). Recently the

^{*} E-mail: regan@ast.cam.ac.uk

<i>Sim</i>	<i>Boxsize</i> [Comoving h^{-1} Mpc]	z_{init}	z_{coll}	<i>DM mass</i> [M_{\odot}]	ΔR [pc]
A	5.0	200.0	15.0	9.58×10^3	9.59×10^{-3}
B	2.0	250.0	14.0	4.42×10^2	1.61×10^{-2}
C	2.0	250.0	15.0	4.42×10^2	1.61×10^{-2}
D	10.0	175.0	15.0	5.52×10^4	1.04×10^{-2}
E	0.5	250.0	-	6.90×10^0	1.00×10^{-1}

M_{tot} [M_{\odot}]	R_{200} [kpc]	V_{200} [km sec $^{-1}$]	T_{vir} [K]	ρ_{max} [cm $^{-3}$]	λ	T_{core} [K]
2.64×10^8	1.28×10^3	29.94	32276.80	1.24×10^9	0.031	6.11×10^3
5.37×10^7	0.64×10^3	18.99	12986.78	5.86×10^8	0.026	6.35×10^3
5.15×10^7	0.59×10^3	19.33	13455.27	7.12×10^8	0.050	6.13×10^3
9.75×10^8	2.18×10^3	51.53	95412.04	7.64×10^5	0.019	6.45×10^3
9.27×10^5	0.13×10^3	5.52	1098.07	5.17×10^0	0.026	1.34×10^3

Table 1. Basic properties of the three simulations (A, B and C) presented in RH08 along with those of two further simulations (D and E): boxsize(comoving h^{-1} Mpc), starting redshift, collapse redshift, DM particle mass (M_{\odot}), spatial resolution (h^{-1} pc), total mass of the halo (M_{\odot}), the virial radius (h^{-1} pc), circular velocity (km sec $^{-1}$), virial temperature (K), maximum baryon density in the halo (cm $^{-3}$), angular momentum parameter λ , and temperature at the core of the halo (K). All units are physical units, unless explicitly stated otherwise.

advent of adaptive mesh refinement (AMR) simulations has enabled numerical simulations of atomic hydrogen driven collapse with a much improved dynamic range. Wise et al. (2007) and Regan & Haehnelt (2008, RH08) used the AMR code ENZO (Bryan & Norman 1995, 1997; Norman & Bryan 1999; O’Shea et al. 2004) to perform numerical simulations of the collapse of metal-free gas at the centre of dark matter haloes with virial temperatures of $\gtrsim 10000$ K in a cosmological context. Both groups found that the gas collapses isothermally, becomes self-gravitating and settles into a close to isothermal density profile within the DM halo. Wise et al. (2007) pushed the resolution of their simulations to study the evolution of the innermost mass shells at the very centre of the halo reaching sub-Jupiter mass scales. RH08 instead followed the dynamical evolution of a much larger fraction of the gas in the halo until it settled into rotational support. RH08 found that between 0.1% and 1% of the gas at the centre formed a massive self-gravitating disc. The discs are surrounded by the ongoing isothermal collapse of the outer mass shells which their simulations were not able to follow due to the prohibitively short dynamical timescales in the dense regions of the disc at the centre of the haloes. The simulations contain a wealth of information regarding the loss of angular momentum and mass in-fall rates during the isothermal collapse in these haloes. We here discuss the implications for the expected further dynamical evolution of the gas.

In §2 we will summarize the main numerical results from RH08, discuss the stability of the self-gravitating discs which have formed and critically assess the assumption that H_2 and metal cooling may be suppressed in (some) pre-galactic haloes with virial temperatures close to but above the threshold for atomic hydrogen cooling driven collapse. In §3 we use the dynamical evolution of the gas settling into rotational support in our simulations to make an educated guess about the further dynamical evolution of the gas in the mass shells outside of the discs which are still undergoing collapse at the end of our simulations. In §4 we discuss the implications for the formation of massive

seed black holes and for the early growth of supermassive black holes. In §5 we discuss our results and conclusions.

2 AMR SIMULATIONS OF ATOMIC HYDROGEN DRIVEN ISOTHERMAL COLLAPSE

2.1 The numerical setup

The setup of the numerical simulations used here is described in detail in RH08. We will give here a brief summary of the salient properties of the simulations. The simulations were performed using the adaptive mesh refinement (AMR) code ENZO originally developed by Greg Bryan and Mike Norman at the University of Illinois (Bryan & Norman 1995b, Bryan & Norman 1997, Norman & Bryan 1999, O’Shea et al. 2004). We used ENZO in its AMR mode to simulate the collapse of the gas at the centre of DM haloes with virial temperatures in the range 13000 – 32000 K assuming that metal and H_2 cooling were suppressed. The three simulations of haloes with virial velocities of 19, 20 and 29 km sec $^{-1}$ described in RH08 will form the basis of our study here. The haloes were selected from simulations with box-sizes of 2.0–5.0 h^{-1} Mpc. The haloes were resolved with ~ 30000 to ~ 120000 DM particles and the simulations were run with the maximum refinement level set to 18 (simulation A) and 16 (simulations B & C) corresponding to a maximum spatial resolution of ~ 0.01 pc in each simulation. Further properties of the simulated haloes are listed in table 1. In the table the reader will also find the properties of two further simulations with smaller and bigger virial temperatures/velocities which will be discussed in §4.5.

2.2 Properties of the Isothermal Collapse

The gas at the centre of the DM haloes cools to a temperature of 7000 – 8000 K due to atomic hydrogen cooling and settles isothermally into a close to $\rho \propto r^{-2}$ profile as shown

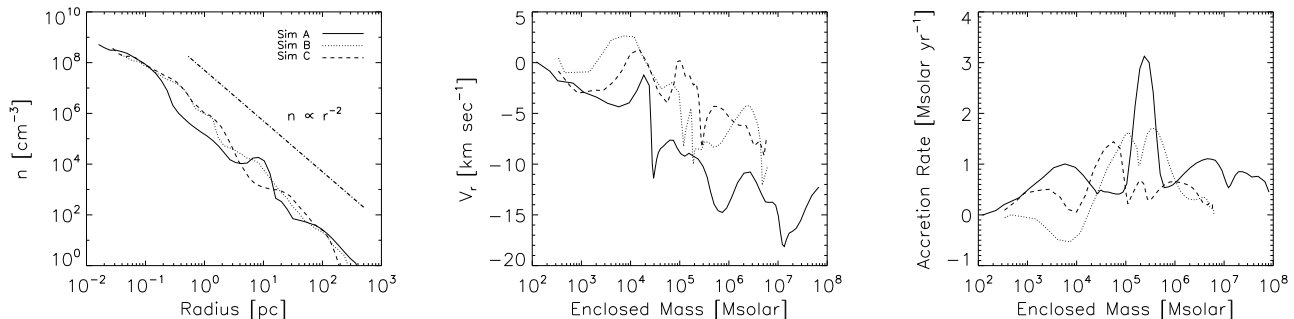


Figure 1. *Left-hand Panel:* The density as a function of radius for simulations A, B & C. The profile is close to isothermal ($n \propto r^{-2}$) over several decades in radius. *Middle Panel:* The radial velocity as a function of enclosed gas mass. Notice the sharp drop in the radial velocity at the mass of the disc in each simulation. *Right-hand Panel:* The mass in-fall rate for each simulation calculated from the density and radial velocity.

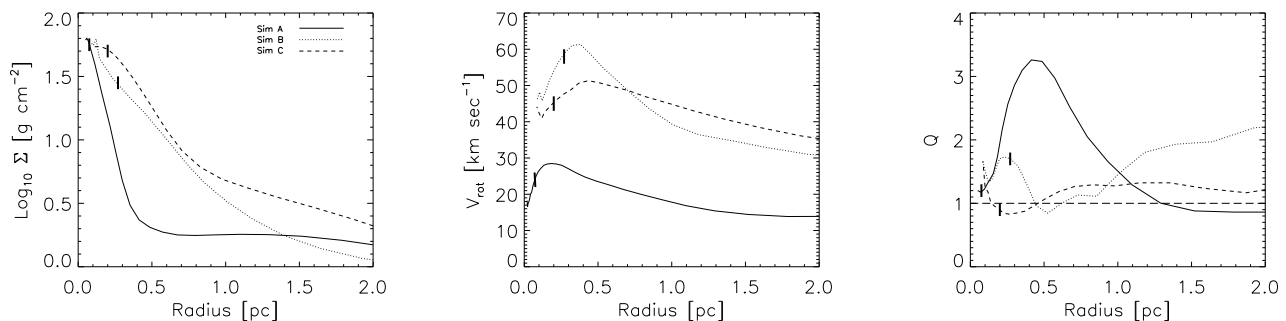


Figure 2. *Left-hand Panel:* The surface mass density of the disc in simulations A-C. Note the exponential density profile within the disc. *Middle Panel:* The rotational velocity of the gas. *Right-hand Panel:* The Toomre parameter, Q , for the gas in the discs. A value of $Q > 1$ (marked with the long dashed line) indicates that the disc is gravitationally stable. The tick marks in each figure indicate the scale radii of the discs.

in the left panel of Figure 1 for simulations A-C. During the collapse, the gas develops supersonic turbulent motions of order the virial velocity of the DM haloes. The gas efficiently loses angular momentum and settles towards the centre with radial velocities, V_r , of $5 - 15 \text{ km sec}^{-1}$ about a factor 3-5 smaller than the virial velocity of the haloes (middle panel of Figure 1). The corresponding mass accretion rates can be estimated as

$$\dot{M} = 4\pi r^2 \rho(r) V_r(r), \quad (1)$$

where $\rho(r)$ is the density at radius r . The mass accretion rates range from a few tenths to about two solar masses per year (right panel of Figure 1).

The central regions in each halo settle into rotational support and form compact, fat, self-gravitating discs with a mass of $\sim 2 \times 10^4 M_\odot$ (simulation A) and $\sim 1 \times 10^5 M_\odot$ (simulations B and C). Note that there is a significant drop in the radial velocity of the gas at the mass shell marking the outer boundary of the discs. The peaks in the mass accretion rate profiles at mass shells outside of the discs are due to clumps of high density gas within the gas surrounding the discs.

In Figure 2 we summarize the basic properties of the discs. The discs in simulations A-C have an exponential surface mass density profile with scale length of 0.075, 0.2 and

0.27 pc, respectively (left panel). In the middle panel of Figure 2 we present the rotation curves of the discs which show peak rotation velocities in the range from $25 - 60 \text{ km sec}^{-1}$. Note that the discs have an elliptical shape and are somewhat fatter than expected for an ideal isothermal exponential disc due to their unrelaxed dynamical state.

3 THE FURTHER DYNAMICAL EVOLUTION OF THE GAS

3.1 Stability and further dynamical evolution of the discs

9

We were able to follow the dynamical evolution of the discs for several rotation periods and the discs appeared not to fragment during this time. The stability of self-gravitating discs is governed by the stabilizing forces of pressure on small scales and rotation on large scales. The gravitational stability of discs is normally characterized by the Toomre parameter (Toomre 1964),

$$Q(r) = \frac{c_s \kappa}{\pi G \Sigma}, \quad (2)$$

where c_s is the sound speed, $\kappa = \sqrt{2}(V_{\text{rot}}/r)(1 +$

$d \ln V_{\text{rot}}/d \ln r)^{1/2}$ (Binney & Tremaine 1987; Oh & Haiman 2002) is the epicyclic frequency, V_{rot} is the rotational velocity, Σ is the surface mass density and r is the radius. For values of $Q < 1$ the disc is expected to be gravitationally unstable. In the right panel of Figure 2 we show the Toomre parameter as a function of radius for the three discs in simulations A-C. Within a few scale radii the discs all have $Q \gtrsim 1$. The Toomre criterion thus predicts that the discs are marginally stable and do not fragment confirming the visual impression from the simulations. The further disc evolution should be governed by the viscous time scale.

In the framework of modelling the viscous evolution of a self-gravitating disc as an α disc (Shakura & Syunyaev 1973) the viscous time scale can be approximated as $t_{\text{visc}} = \alpha^{-1}(H/R)^{-\beta}t_{\text{dyn}}$, where t_{dyn} is the dynamical time, (H/R) is the ratio of disc height to the radius of the disc and $\beta = 2$ for a geometrically thin disc (Lin & Pringle 1987). The discs in our simulations are rather fat with $(H/R) \sim 0.2 - 0.3$ and the “effective” beta is probably somewhat smaller than 2. Initially the α parameter should be of order 0.1 for the marginally stable discs (Lin & Pringle 1990). The viscous timescale on which the disc evolves should therefore be a few tens of dynamical times. Due to the viscous evolution angular momentum will be transported outwards. The discs will contract, the rotation velocity will increase and gas pressure support will decrease making the discs more violently unstable. The α parameter will thus increase rapidly to order unity and the discs will stay fat due to the turbulent motions induced by gravitational instabilities. Outward angular momentum transport will continue, perhaps, supported by the bars-in-bars mechanism proposed by Shlosman et al. (1989, 1990) (see Begelman et al. (2006, 2008) for a discussion in this context). The viscous timescale will then be locked at a few times the ever decreasing dynamical time scale.

3.2 The suppression of metal and H_2 cooling and the role of star formation

The most critical assumption in our numerical simulations is that cooling by atomic hydrogen and helium is dominant which prevents the gas from cooling below ~ 7000 K. The temperature of the gas close to the virial temperature of the halo is the reason that no efficient fragmentation has taken place in the simulations and will presumably also not occur during the further collapse of the outer mass shells. The temperature of the gas is close to the virial temperature of the discs which is important for their stability. Cooling by atomic hydrogen and helium is only dominant when the H_2 and metal abundances are very small. We will now discuss the plausibility of this assumption for H_2 and metals in turn.

At the densities of the gas in our simulations the H_2 formation timescale is generally shorter than the dynamical scale. In the absence of a strong ultra-violet (UV) flux H_2 should form with a universal abundance of $x_{H_2} \approx 10^{-3}$ (Oh & Haiman 2002). Efficient dissociation of H_2 is thus necessary for our assumption, that atomic cooling is dominant, to be valid.

H_2 molecules can be dissociated by ultra-violet radiation, either directly by photons with energies greater than 14.7 eV or as a result of electronic excitation in the Lyman-Werner (LW) bands ($11.2 \text{ eV} < E < 13.6 \text{ eV}$). Omukai

& Nishi (1999), Glover & Brand (2001), Oh & Haiman (2002), Bromm & Loeb (2003) and Dijkstra et al. (2008) have all discussed in considerable detail H_2 formation and dissociation in haloes similar to the ones we have simulated here. UV photons in the LW bands have substantially longer mean free paths and should thus be more important for the dissociation of molecular hydrogen. Efficient dissociation of molecular hydrogen requires a UV flux of $F_{21, LW} \gtrsim 1000$ (Bromm & Loeb 2003), where F_{21} is in units of $10^{21} \text{ erg s}^{-1} \text{ cm}^{-2} \text{ Hz}^{-1} \text{ sr}^{-1}$. Dijkstra et al. (2008) have suggested that there may exist a small fraction of haloes close to a neighbouring actively star-forming halo where the external UV background reaches this critical flux. However, they estimate this fraction to be very small, a few times 10^{-7} . More important is therefore probably internal UV radiation produced within the haloes. Omukai & Nishi (1999), Glover & Brand (2001) and Oh & Haiman (2002) argue that as little as one massive star could in principle be sufficient to dissociate the entire molecular hydrogen content of our haloes. The gas in the discs have rotational velocities of $30 - 50 \text{ km sec}^{-1}$ and the gas should thus sit in sufficiently deep potential wells to withstand the feedback effects due to the resulting supernovae.

The second assumption we have made in our simulations is that the halo is virtually metal-free. It is not clear at what metallicity metal cooling would become important for our simulations. Omukai et al. (2008) have used one-zone models to study this problem and found that a critical metallicity of $Z_{\text{cr}} \geq 5 \times 10^{-6} Z_{\odot}$ leads to a sufficiently soft equation of state to allow fragmentation via dust cooling at densities of $n \sim 10^{10} \text{ cm}^{-3}$, somewhat higher than the highest densities in our simulations. In the absence of dust the critical metallicity rises to $Z_{\text{cr}} \geq 3 \times 10^{-4} Z_{\odot}$ above which fragmentation can occur at substantially lower densities. It is unclear to what extent metals produced by stars would actually mix with the gas. If the gas in the haloes were efficiently enriched with metals fragmentation is obviously expected to occur. However, it is then still unclear how efficient fragmentation and star formation would be. Even if the gas in the majority of haloes with $T_{\text{vir}} \gtrsim 10000 \text{ K}$ fragments and forms an ordinary star cluster a small fraction of haloes with the right conditions to justify our assumption of cooling to be dominated by atomic cooling may be all that is needed to produce the seeds for the much smaller number of SMBHs.

3.3 Further dynamical evolution of the outer mass shells

The discs in our simulations sit at the centres of the ongoing collapse of the gas in the DM haloes. Unfortunately the dynamical timescales in dense regions of the discs have become prohibitively short and our simulations are thus not able to follow the further dynamical evolution of the outer mass shells. As discussed in more detail in RH08 the gas in the outer parts of the haloes are neither supported by thermal pressure nor by rotation. The gas is instead marginally supported by turbulent pressure and should thus settle further until it either fragments or reaches rotational support. We will now investigate at which radius we should expect rotational support to set in for the gas in the outer mass shells.

In the left hand panel of Figure 3 we show an estimate

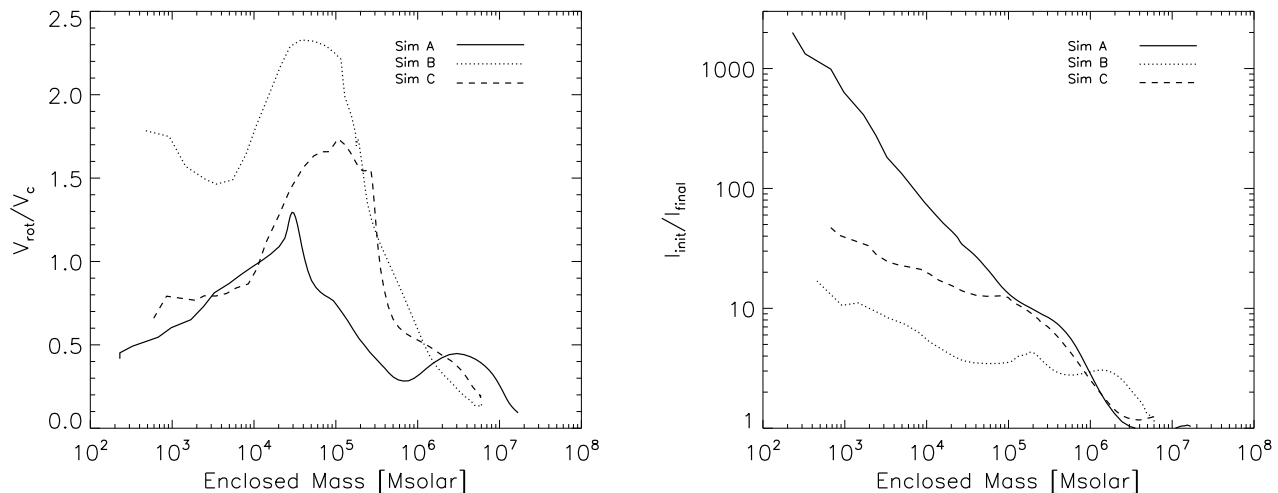


Figure 3. *Left-hand Panel:* The ratio of the rotational velocity, estimated using the inertia tensor (see RH08 for details), to circular velocity, V_c . The ratio peaks at the enclosed mass of the disc. A value of $\gtrsim 1.0$ indicates rotational support. *Right-hand Panel:* The ratio of the initial angular momentum, l_{init} , to the final angular momentum, l_{final} .

of the level of rotational support as a function of enclosed mass at the end of the simulation. The figure shows the ratio of an estimate of the rotational velocity based on the the inertia tensor of the gas (see RH08 for details) and the circular velocity, V_c . As expected the ratio peaks at the enclosed mass of the rotationally supported discs for each of the simulations. Note that in simulation B the ratio peaks at an somewhat high value of ≈ 2.4 due to the complex dynamical interactions of two clumps in a multiple clump system. In the following we will take a ratio of 1.5 as indicative of rotational support.

In the right hand panel of Figure 3 we show the ratio of the initial angular momentum to the final angular momentum as a function of enclosed mass. We choose as the initial value of the angular momentum in each simulation the value at the time when the maximum refinement level reached is 15 in simulation A and 12 in simulations B & C at which time the mass shells in question are sufficiently resolved.

The loss of angular momentum varies between a factor of 10 and a factor of 2000 for simulations A to C. Towards the outer mass shells the angular momentum loss by the end of the numerical simulation becomes progressively smaller due to the increasing dynamical time at larger radii.

We first calculate the radius the outer mass shells would collapse to if angular momentum were conserved. As the gas in a given mass shell has been losing angular momentum rapidly up to the end of the simulation this is unlikely to be the case but should give an upper limit for the radius at which rotational support is reached. If rotational support is reached for $V_{\text{rot}}(R_{\text{sup}}) = 1.5V_c(R_{\text{sup}})$ and angular momentum is conserved the final radius of a mass shell with enclosed mass, M , is related to the radius at the end of the simulation, R_{sim} , as,

$$R_{\text{sup}} = \left[\frac{V_{\text{rot}}(R_{\text{sim}})}{V_{c,\text{gas}}(R_{\text{sim}}) \times 1.5} \right]^2 \times R_{\text{sim}}. \quad (3)$$

Note that at the largest radii the gas has not yet become self-gravitating at the end of the simulation so $V_{c,\text{gas}}(r_{\text{sim}}) =$

$\sqrt{GM_{\text{gas}}/r_{\text{sim}}}$ is calculated for the gas mass only. When rotational support is reached the gas is always self-gravitating. In the left hand panel of Figure 4 we compare the radius as a function of enclosed mass at the end of the simulation (black curves) with the radius when rotational support is reached as given by equation 3 (red curves). Note that for the mass shells within the discs our estimate for the radius of rotational support can be larger than the actual radius at the end of the simulation due to our assumption $V_{\text{rot}}(R_{\text{sup}}) = 1.5V_c(R_{\text{sup}})$ which is exceeded in some parts of the disc.

The gas in the outer mass shells is still rapidly losing angular momentum at the end of the simulations. We have not fully understood the angular momentum loss mechanism yet but it appears that shocks due to the supersonic turbulent motions lead to the dissipation of energy and a redistribution of angular momentum which is presumably efficiently transported outwards (Wise et al. 2007). As we know little yet about the details of this process we can only speculate about the further angular momentum loss of the gas in the outer mass shells. In the right hand panel of Figure 4 we plot the radius the gas would collapse to if the gas in all mass shells loses the same fraction of angular momentum as that in the outermost mass shell of the disc which has formed in the respective simulation. The radius where rotational support sets in is then given by

$$R_{\text{sup}} = \left[\beta(M) \frac{V_{\text{rot}}(R_{\text{sim}})}{V_{c,\text{gas}}(R_{\text{sim}}) \times 1.5} \right]^2 \times R_{\text{sim}}, \quad (4)$$

where $\beta(M)$ is the extra fraction of angular momentum that must be lost by the outer mass shells so that their angular momentum loss is the same as that angular momentum lost by the gas which is rotationally supported at the disc radius. For mass shells within the disc radius we set $\beta(M) = 1$.

In order to get a feel for how compact the configuration of the gas in our simulations is compared to observed astrophysical objects we also show the typical masses and radii of observed compact nuclear star clusters, globular

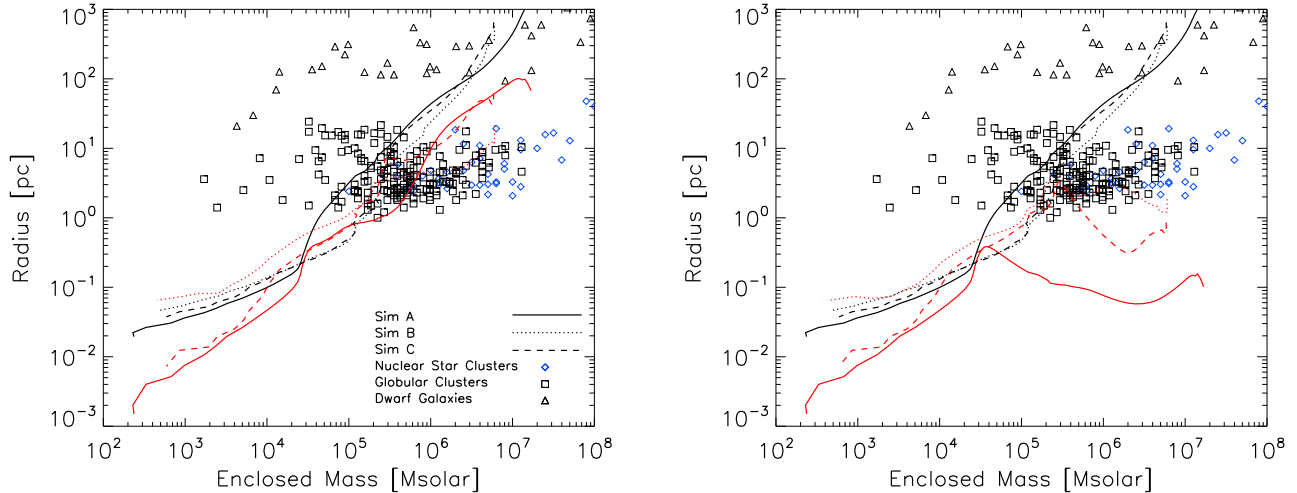


Figure 4. *Left-hand Panel:* The black curves show the enclosed gas mass as a function of radius at the end of simulation A-C. The red curve show the radii to which the gas will fall if the gas becomes rotationally supported with $V_{\text{rot}}(R_{\text{sup}}) = 1.5 \times V_c(R_{\text{sup}})$ and angular momentum is conserved. *Right-hand Panel:* In this case the red curves show the radius to which the gas will fall if we assume the gas becomes rotationally supported with $V_{\text{rot}}(R_{\text{sup}}) = 1.5 \times V_c(R_{\text{sup}})$ and the gas loses the same fraction of angular momentum as the gas which has settled into rotational support in the disc at the end of the simulations. The blue diamonds give masses and radii of a sample of observed compact nuclear star clusters as given by Merritt (2008). The black squares and triangles give masses and radii inferred for globular clusters and dwarf galaxies based on data from Belokurov et al. (2007).

clusters, and dwarf galaxies (Belokurov et al. 2007; Merritt 2008; Seth et al. 2008). We assume a mass-to-light ratio of 5 when converting the luminosities in Belokurov et al. (2007) to masses.

Due to the efficient loss of angular momentum the gas in our simulations settles into rotational support in a substantially more compact configuration than the stellar component of nearby dwarf galaxies which are hosted by DM haloes with virial velocities similar to the ones we have simulated here, albeit obviously at $z = 0$ instead of $z = 15$. At the same mass the radii are typically one to three orders of magnitude smaller. Observed globular cluster and nuclear star cluster are more compact and are generally hosted by galaxies/DM haloes much more massive than the DM haloes we are considering here making a comparison less straightforward. The inner mass shells ($\lesssim 10^5 M_\odot$) of the gas in our DM haloes settle into a configuration which is also substantially (by an order of magnitude in radius) more compact than globular clusters of the same mass. The configuration of the gas in the outer mass shells is expected to settle into rotational support at radii which are similar or smaller than those of compact nuclear star clusters depending on how much angular momentum loss will occur. Note, however, that the observed clusters may have expanded due to the rapid removal of gas (Bastian & Goodwin 2006).

4 IMPLICATIONS FOR THE FORMATION OF MASSIVE SEED BLACK HOLES

4.1 Pathways to a massive black hole

Various mechanisms by which a massive black hole may form have been laid out comprehensively by Rees (Rees 1978, 1984). Since then considerable effort has gone into

researching the paths in this flow chart but the actual formation process of SMBH nevertheless still eludes us. Figure 5 summarizes the paths to a massive black hole concentrating on the possibilities that pre-galactic DM haloes with $T_{\text{vir}} \gtrsim 10000 \text{ K}$ offer. We thereby use the results of our numerical simulations as a starting point. In the now well established hierarchical paradigm for galaxy formation (White & Rees 1978) DM haloes with $T_{\text{vir}} \gtrsim 10000 \text{ K}$ build-up through the merging of several DM haloes with smaller virial temperatures. In these less massive haloes gas can only collapse and form stars, if the gas cools due to H_2 and/or metals. Especially for the first generation of these haloes it is thus very uncertain, how efficiently they have formed stars (e.g. Greif et al. 2008; Norman 2008; Whalen et al. 2008). As discussed in §3.2 this also introduces considerable uncertainty for the cooling processes and star formation efficiency in the more massive haloes with $T_{\text{vir}} \gtrsim 10000 \text{ K}$. If fragmentation and star formation is efficient early on, an ordinary star cluster/dwarf galaxy may form. If cooling on the other hand is dominated by atomic cooling the gas is expected instead to settle into a rotationally supported, fat, self-gravitating disc (Mo et al. 1998; Oh & Haiman 2002). The further fate of this disc depends crucially on whether atomic cooling remains the dominant cooling process during the further evolution of the disc. If this is the case the gas will not efficiently fragment and will continue to contract on a timescale controlled by the rate at which the gas loses angular momentum. As the gas will be gravitationally unstable this is expected to occur on a timescale which is longer by a factor of a few than the dynamical timescale. The further fate then depends on how efficiently the entropy produced by the release of gravitational en-

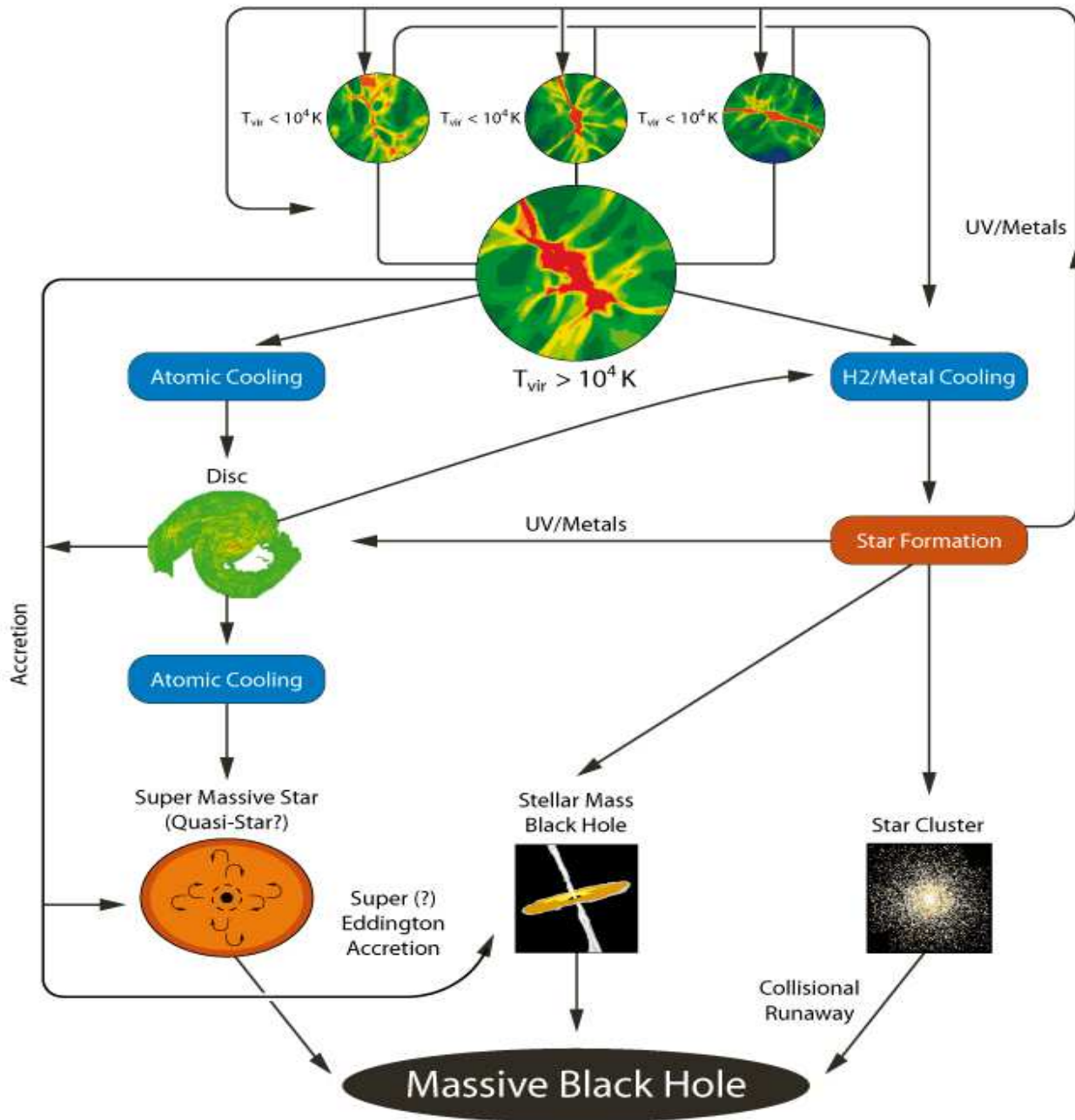


Figure 5. Summary of the possible pathways to massive black holes via a stellar seed black hole, a quasi star or via a nuclear star cluster in DM haloes with $T_{\text{vir}} \gtrsim 10000 \text{ K}$.¹

ergy is trapped. One possibility is that the gas settles into an high entropy super-massive star (e.g. Hoyle & Fowler

¹ The four pictures of simulated haloes at the top of the figure and the disc show simulations described in RH08, the sketch of the quasi-star is based on that in Begelman et al. (2008) and the picture of the star cluster shows the globular cluster M80 (source: <http://hubblesite.org/newscenter/archive/1999/26/image/a>).

1963a,b; Chandrasekhar 1964a,b; Zel'Dovich & Novikov 1967; Zel'Dovich 1970; Shapiro & Teukolsky 1979, 1983) which may take the form of a quasi-star as recently suggested by Begelman et al. (2006). If the released gravitational energy is instead transported away in a disc-jet configuration then rapid accretion onto a stellar mass seed black hole would be the expected outcome. Finally if either metal or H_2 cooling become efficient in the self-gravitating disc and

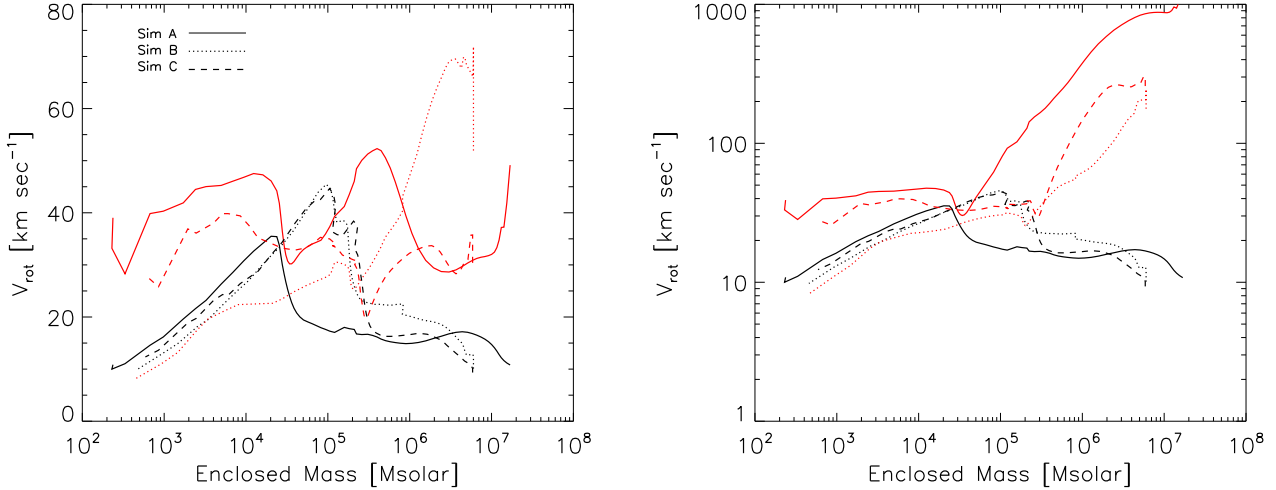


Figure 6. *Left-hand Panel:* The black curves show the rotational velocity as a function of enclosed mass at the end of simulation A-C. The red curves show the rotational velocity the gas attains if it settles into rotational support with $V_{\text{rot}}(R_{\text{final}}) = 1.5 \times V_c(R_{\text{final}})$ and angular momentum is conserved. The values of R_{final} in Figure 4 are used. *Right-hand Panel:* In this case the red curves show the rotational velocity of the gas attains if we assume the gas reaches rotational support with $V_{\text{rot}}(R_{\text{final}}) = 1.5 \times V_c(R_{\text{final}})$ and loses the same fraction of angular momentum as the gas which has settled into rotational support in the disc at the end of the simulations. The values of R_{final} in the right hand panel of Figure 4 are used in this case.

fragmentation is efficient a very compact star cluster should form (e.g. Omukai et al. 2008; Bernadetta & Volonteri 2008). In the following we will discuss these different possibilities in more detail.

4.2 Super-massive stars and quasi-stars

At the time when the gas settles into rotational support in our simulation the surface mass density at the center exceeds 30 g/cm^2 (Figure 1) and the gas is thus optically thick. The dominant energy production process is the release of gravitational energy. As argued in §3.1 this will occur on a few times the dynamical time scale. The corresponding mass inflow rate and luminosity rise rapidly as the gas contracts. They can be estimated as $\dot{M} \sim 0.1 v_c^3/G \sim 1 (v_c/30 \text{ km sec}^{-1})^3 M_\odot \text{ yr}^{-1}$ and $L_{\text{grav}} \sim 0.1 v_c^5/G \sim 3.6 (v_c/30 \text{ km sec}^{-1})^5 \times 10^{38} \text{ erg s}^{-1}$. If the gas in the discs in our simulations is able to contract by another factor 100 in radius without efficient fragmentation the circular velocity will rise to 300 km sec^{-1} . At this stage the luminosity due to the release of gravitational energy will become comparable to the Eddington luminosity L_{Edd} , where the outward pressure due to the radiation balances the gravitational attraction,

$$L_{\text{Edd}} = \frac{4\pi GMm_H c}{\sigma_T} \simeq 1.3 \times 10^{43} \left(\frac{M}{10^5 M_\odot} \right) \text{ erg s}^{-1}, \quad (5)$$

where c is the speed of light, m_H is the mass of a hydrogen atom and σ_T is the Thomson scattering cross-section.

If the entropy produced due to the release of gravitational binding energy can be trapped in a quasi-spherical configuration the disc should puff up (e.g. Begelman & Rees 1978) when the luminosity due to the release of gravitational binding energy exceeds the Eddington luminosity and a (radiation) pressure supported super-massive star should

ensue. Begelman et al. (2006, 2008) have argued that a supermassive star embedded in a spherical accretion flow with mass accretion rates in the range $\sim 0.1 - 1 M_\odot \text{ yr}^{-1}$ will develop a core-envelope structure akin to that of a Thorne-Zytkow object where a compact neutron star is embedded in a diffuse red giant star (Thorne & Zytkow 1977).

Begelman et al. (2006) dubbed such an object a “quasi-star” and envisage its evolution as follows. Initially a compact core of about $10 - 20 M_\odot$ surrounded by a more diffuse radiation-pressure supported envelope forms. In the central regions nuclear reactions may commence but the corresponding energy release is not expected to exceed the release of gravitational binding energy. The high mass in-fall rate continues to compress and heat the core. Begelman et al. (2008) argue that the core can reach temperatures of up to $5 \times 10^8 \text{ K}$ at which point the gas should cool catastrophically due to thermal neutrino cooling leading to a core-collapse black hole. At this stage the black hole is surrounded by a massive gas envelope of more than one hundred times the mass of the black hole and the central black hole accretes at a rate which corresponds to the Eddington rate of the mass in the envelope. Given that the mass of the envelope is much larger than the mass of the black hole this allows the black hole to quickly grow to a mass of $10^3 - 10^4 M_\odot$, at which point Begelman et al. (2008) argue the quasi-star evaporates as the photospheric temperature falls. Whether this is actually the correct picture is still rather uncertain but definitely merits further investigation. It is, however, interesting to note that the postulated in-fall rates in the Begelman et al. model are similar to those in our simulations. The in-fall rates of the gas in the outer mass shells at the end of our simulations range from $0.3 - 1.5$ solar masses per year and as we have discussed at the start of this section the inflow rates at the centre of the discs, which have formed in our simulations, are expected to become even larger as

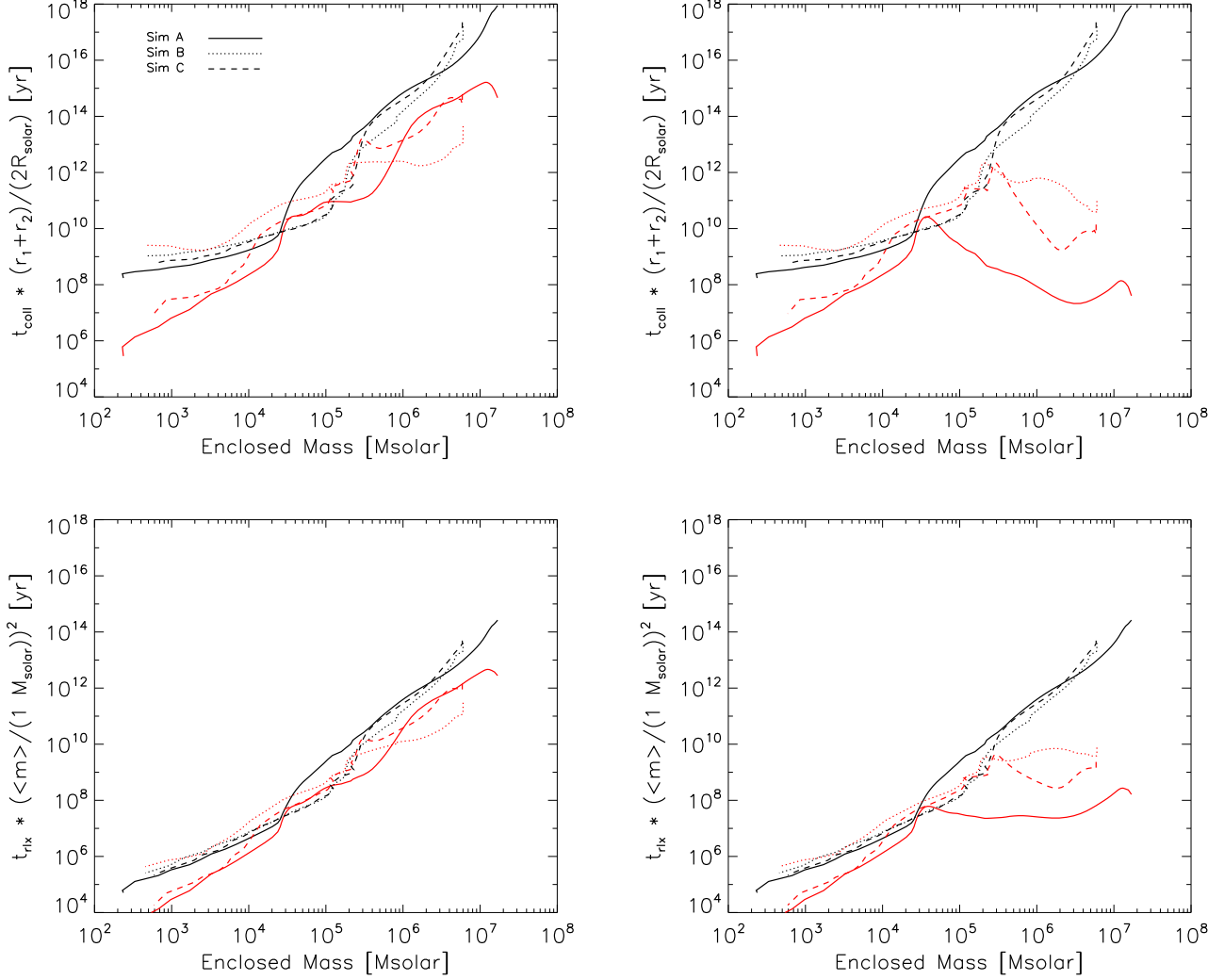


Figure 7. *Top Panel: Left-hand Panel:* The black curves show the expected collision times (equation 6) for stellar collisions in a compact star cluster with masses and radii as that of gas at the end of simulation A-C. The red curves are the expected collision times assuming that the gas settles into rotational support without losing further angular momentum using the values of R_{final} from the left hand panel of Figure 4. *Right-hand Panel:* The collision times assuming that further angular momentum is lost as described in section 3.3 and using values of R_{final} as in the right hand panel of Figure 4. *Bottom Panel:* The same plots except in this case the relaxation time (equation 7) is plotted against enclosed mass.

the self-gravitating discs evolve on a viscous timescale due to gravitational instabilities.

4.3 Super-Eddington accretion of stellar mass black hole seeds

If some star formation occurs in the discs at the centre of our haloes a stellar mass black hole with a mass of up to $100 M_{\odot}$ should easily form. Alternatively a stellar mass black hole which has formed in the early stages of the collapse or in one of the precursors of our DM haloes may sink to the centre of the DM potential in which our discs form. Independent of whether a supermassive star will form from the gas settling to the centre of the disc such black holes find themselves in an ideal environment for rapid growth. The surrounding material is flowing to the centre at highly super-Eddington

accretion rates compared to the Eddington accretion of a stellar mass black hole. The rotational velocities of our discs range from $30 - 60 \text{ km sec}^{-1}$ and the material is thus already strongly bound. The energy released by a stellar mass black hole will not be able to halt the surrounding inflow of matter and the black hole should grow quickly at highly super-Eddington rates to masses comparable to the disc masses if fragmentation is not important. In Figure 6 we plot the rotational velocities at which the outer mass shells are expected to settle into rotational support for our two assumptions regarding angular momentum loss. If the gas in the outer mass shells lose angular momentum as efficiently as the gas in the discs in our simulations the rotational velocity could be as large as several hundred km sec^{-1} . This is quite remarkable considering that the virial velocities of the DM haloes are in the range $20 - 30 \text{ km sec}^{-1}$. There is thus potential for

rapid further growth and the final black hole mass would probably be set by competition between gas consumption by star formation and accretion for the outer mass shells or by the increasing feedback due to the increasing accretion luminosity.

If the entropy produced due to the release of gravitational energy during the accretion is trapped in a quasi-spherical configuration then the accreting black hole would actually be very similar to the later stages of a supermassive star discussed in the last section. The released gravitational energy may, however, not efficiently couple to the surrounding inflowing matter. It could instead be transported outwards in the form of a jet as is observed in young stars, active galactic nuclei and probably also gamma ray bursts (e.g. Mundt et al. 1990; Begelman et al. 1984; Mészáros & Rees 2001). Accretion would then occur in a fat accretion disc at super-Eddington accretion rates possibly involving the photon bubble instability (Gammie 1998; Turner et al. 2005) and/or advection dominated in-/outflows as discussed by Blandford & Begelman (1999) and Begelman (2001).

4.4 The formation and evolution of a compact star cluster

As briefly discussed in §3.2 the evolution of the gas in dynamical haloes with virial temperatures $T_{\text{vir}} \gtrsim 10000$ K depends crucially on whether metals and/or H_2 are present in sufficient abundance to facilitate cooling well below the virial temperature. If this is the case the gas at least in principle can fragment and form stars, even though it is unclear how efficient fragmentation and star formation in this situation would be (e.g. Omukai et al. 2008). If star formation occurs early on in the collapse the outcome is probably similar to nearby dwarf galaxies, which have DM haloes of similar virial velocity and temperature as those we have found in our simulations. Some of the nearby dwarf galaxies should have actually formed at similarly high redshifts ($z \sim 15$) as we are discussing here. Early fragmentation requires the presence of a substantial metallicity and most likely also dust. Dwarf galaxies have typical metallicities of a hundredth to a tenth of solar. Star formation appears to be very inefficient in dwarf galaxies. This is generally assumed to be due to feedback from supernovae and or ionizing radiation which appears to strongly affect star formation in haloes with $V_c \lesssim 50$ km sec $^{-1}$.

It seems, however, likely that at $z \sim 15$ (and perhaps even at the present day) a fraction of DM haloes with virial temperatures $T_{\text{vir}} \gtrsim 10000$ K have not yet been significantly polluted with metals or that the metals in them have not been sufficiently mixed into the cold gas phase for metal cooling to be relevant.

In such haloes stars could probably only form by H_2 cooling once rotational support has set in. As discussed in §4.1 this would lead to very compact star clusters which may well be substantially more compact (see Figure 4) than the globular clusters and the compact nuclear star clusters which have been discovered in the centres of many galaxies including luminous elliptical galaxies and the bulges of spiral galaxies thanks to the unrivaled resolution of the Hubble Space Telescope (e.g. Carollo et al. 1997, 1998; Böker et al. 2002; Côté et al. 2006).

If the gas in our haloes were to fragment and form a

star cluster, after rotational support sets in, then the typical velocity dispersions of the star cluster would be substantially larger than the velocity dispersion of the DM haloes which host them and could in principle reach several hundred km sec $^{-1}$ if the outer mass shells lose angular momentum as efficiently as the gas in the discs in our simulations.

Runaway collision at the the centre of dense stellar systems is another promising pathway to the formation of a massive black hole which has been studied intensively (Begelman & Rees 1978; see Freitag (2008) for a review and further references). For a stellar cluster with density n_* and velocity dispersion $\sigma_{\text{rel}}^2 = \sigma_1^2 + \sigma_2^2$ with two populations of stars with stellar masses m_1 and m_2 and stellar radii r_1 and r_2 the collision time can be estimated as, (Binney & Tremaine 1987; Freitag 2008)

$$t_{\text{coll}} \simeq 5 \text{ Gyr} \frac{1 \times 10^6 \text{ pc}^{-3}}{n_*} \frac{\sigma_{\text{rel}}}{10 \text{ km sec}^{-1}} \frac{2 R_{\odot}}{r_1 + r_2} \frac{2 M_{\odot}}{m_1 + m_2}. \quad (6)$$

In Figure 7 we show this estimate for the collision time scale of putative star clusters forming when the gas would settle into rotational support in our simulations for our two assumptions regarding the loss of angular momentum. We take $3M/4\pi R^3$ as a proxy for the stellar mass density and estimate σ_{rel} as $V_c/\sqrt{2}$. For solar mass stars the collision timescales for a star cluster, with mass and radius similar to that expected for the gas in our simulations if it continues to loose angular momentum, could become shorter than the Hubble time ($\sim 4.16 \times 10^8$ yr at $z = 15$).

Stars in a populous cluster ($N \gg 10$) exchange energy and angular momentum through two-body relaxation. The result of this relaxation process is the efficient mass segregation of the cluster with more massive stars concentrated at the centre of the cluster and a much enhanced central density (e.g. Spitzer 1969; Binney & Tremaine 1987) which eventually can lead to core collapse. The estimate in Figure 7 will thus be a substantial overestimate for the collision time of the central regions of such a cluster especially if core collapse has occurred.

The relaxation time can be estimated as in Freitag (2008),

$$t_{\text{rlx}} = 2 \text{ Myr} \frac{10}{\Lambda} \frac{10^6 \text{ pc}^{-3}}{n_*} \left(\frac{\sigma_{\text{rel}}}{10 \text{ km sec}^{-1}} \right)^3 \left(\frac{1 M_{\odot}}{\langle m \rangle} \right)^2 \quad (7)$$

where $\Lambda \simeq \ln(0.02 N)$, N is the number of stars in the cluster and $\langle m \rangle$ is the mean stellar mass. The timescale for core collapse to occur is a few times the relaxation timescale at the centre of the cluster. If the timescale for core collapse is shorter than the main sequence life time of massive stars a very massive star should form by collisional runaway collapse (Gürkan et al. 2006; Portegies Zwart et al. 2004).

In the bottom panel of Figure 7 we have plotted the relaxation time for our two assumptions of angular momentum loss. The central relaxation time scale and thus the time scale for core collapse of a putative cluster will again be substantially smaller than this. Conditions for the formation of a very massive star by collisional runaway and a subsequent collapse to a massive black hole appear thus to be favourable especially for stellar clusters in the lower mass range around $10^4 - 10^5 M_{\odot}$ (Freitag 2008). As discussed in §4.3 such a massive black hole would find itself in an ideal environment for rapid further growth.

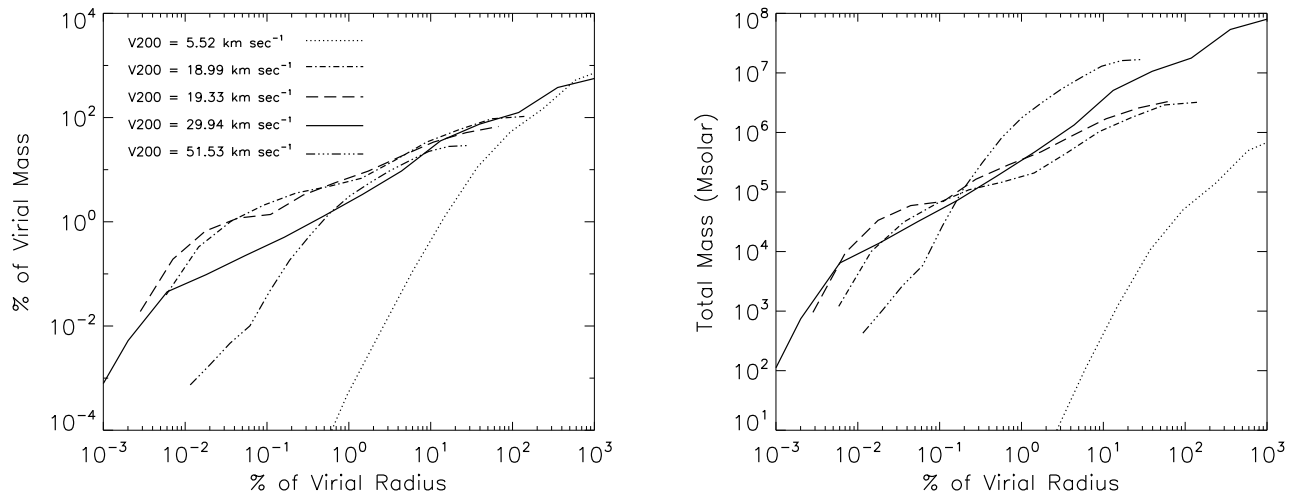


Figure 8. *Left-hand Panel:* The fraction of enclosed mass as a function of the fraction of the virial radius. *Right-hand Panel:* The enclosed mass as a function of the fraction of the virial radius. The collapse into a compact configuration appears to be most efficient in haloes with $V_{\text{vir}} \sim 20 \text{ km sec}^{-1}$ suggesting that massive seed black holes form most efficiently in these haloes. This should imprint a characteristic mass on the mass spectrum of massive seed black holes.

4.5 Characteristic masses of massive black hole seeds

So far we have concentrated on simulations A-C for DM haloes with virial velocities in the range $19 - 30 \text{ km sec}^{-1}$. Recall that the mass of the discs in our simulations are $2 \times 10^4 M_{\odot}$ and $1 \times 10^5 M_{\odot}$. Intriguingly the more massive discs form in the smaller mass haloes. In order to investigate if this is a general trend we have run two further simulations, D and E, for haloes with larger and smaller masses (see table 1 for details) extending the range of virial masses from $\sim 1 \times 10^6 - 1 \times 10^9 M_{\odot}$ which correspond to virial velocities $\sim 6 - 52 \text{ km sec}^{-1}$. Due to the adaptive nature of the Enzo code the spatial resolution and the gas resolution is comparable in all simulations.

The fraction of the mass within a certain fraction of the virial radius at the time when rotational support sets is shown in the left hand panel of Figure 8. It appears to have a maximum for virial velocities around 20 km sec^{-1} .

For lower mass haloes the temperatures attainable by atomic cooling is above the virial temperature of the halo and the gas cannot collapse without efficient metal or molecular hydrogen cooling. Surprisingly for the more massive haloes the collapse also becomes less efficient.

In the right hand panel of Figure 8 we have plotted the total mass against the fraction of the virial radius. The collapse into a compact configuration appears indeed to be most efficient in DM haloes with virial velocities around 20 km sec^{-1} and to lead to the formation of compact self-gravitating discs with characteristic masses of $10^5 M_{\odot}$. This should result in a peak in the mass function of black hole seeds and establish a characteristic mass for the population of massive black hole seeds. Predicting the space density of massive black hole seeds formed in the way discussed here would require to predict the fraction of haloes with $V_{\text{vir}} \sim 20 \text{ km sec}^{-1}$ for which the conditions for the suppression of H_2 and metal cooling are favourable which is beyond

the scope of this paper. However a fraction as small as 0.1% would be sufficient to seed the population of present-day super-massive black holes in galactic bulges.

5 DISCUSSION AND CONCLUSIONS

We have discussed here the pathways to massive black holes in DM haloes with $T_{\text{vir}} \gtrsim 10000 \text{ K}$ based on insights into the formation of self-gravitating compact discs from ENZO AMR simulations of atomic cooling driven collapse in such haloes.

We argue that in a fraction of these haloes the conditions should be just right for a rapid and efficient build-up of massive black holes and rather different from those found in the DM host haloes of dwarf galaxies with similar virial velocities.

For this to be the case the metallicity in the collapsing gas in these haloes has to be sufficiently low for metal cooling not to induce early efficient fragmentation and star formation. The gas can then lose 90% and more of its angular momentum due to supersonic turbulent motions before it first settles into rotational support in a very compact configuration with rotational velocities well in excess of the virial velocity of the DM halo. The corresponding fat, self-gravitating discs are marginally stable against gravitational instabilities.

If at this stage either H_2 or metal cooling induce sufficient fragmentation/star formation a very compact nuclear star cluster would form offering favourable conditions for the formation of an intermediate mass black hole by collisional run-away possibly with the intermediate stage of a super-massive star.

If instead after the onset of rotational support atomic cooling is still the dominant cooling process because the metallicity is still low and H_2 cooling is suppressed due to external or more likely internal UV Lyman-Werner radiation the gas will still be unable to fragment while gravitational

instabilities will induce continued loss of angular momentum.

If the entropy due to the released gravitational energy can thereby be efficiently trapped the geometry of the inflow of gas will stay spherical and a supermassive star will form. The ongoing collapse of the outer mass shells occurs with mass accretion rates of a few tenth to a few $M_{\odot} \text{ yr}^{-1}$. This is just the range of accretion rate for which Begelman et al. (2006, 2008) have suggested that the supermassive star should take the form of a rapidly accreting quasi-star with a pronounced core-envelope structure and a rapidly growing core which will turn into a rapidly growing stellar mass black hole.

If the gravitational binding energy is instead transported away in a disc-jet configuration the accretion flow driven by the in-fall of the outer mass shells is likely to be directed onto a remnant black hole of an ordinary star of which the DM halo should contain at least a few.

In any case the infalling gas becomes strongly bound and has inflow rates which largely exceed the Eddington accretion rate for a stellar mass black hole. Feedback due to individual supernova is expected to have little direct effect on the dynamical evolution of the gas at this stage and rapid growth to a massive black hole is expected.

We have performed numerical simulations for a range of virial velocities from 6 to 52 km sec^{-1} . As expected in DM haloes with $V_{\text{vir}} \lesssim 10 \text{ km sec}^{-1}$ the temperature of the gas attained by atomic cooling only is too low for the gas to collapse. Somewhat surprisingly in the more massive haloes with masses above this threshold the settling of the gas at the centre of the DM haloes becomes rapidly less efficient with increasing mass. If the gas temperature is well below the virial temperature of the DM halo the gas appears to break more easily into several lumps and random motions become more efficient in stabilizing against collapse. DM haloes with virial velocities close to the threshold of $V_c \gtrsim 10 \text{ km sec}^{-1}$ show the largest gas mass settling into a self-gravitating disc.

This suggests that massive seed black holes will form with a characteristic mass. The exact value of this characteristic mass is uncertain but should be set either by the competition of accretion onto the massive black hole and consumption of gas in star formation or by the feedback on the inflow from the energy released in the accretion flow; $10^5 - 10^6 M_{\odot}$ appears to be a likely mass range. The population of massive seed black holes forming in pre-galactic haloes at $z \sim 15$ discussed here will naturally grow into the observed population in observed galactic bulges during the rapid hierarchical build-up of galaxies expected to occur at somewhat smaller redshift. The early formation of such massive black holes strongly alleviates the many problems which have been identified if supermassive black holes had to grow from stellar mass black holes in smaller dark matter haloes or more generally in an environment where supernova feedback from star formation can prevent the supply of sufficient amounts of fuel for rapid growth.

ACKNOWLEDGEMENTS

We thank Mitch Begelman, Giuseppe Lodato, Prija Nataraajan, Jim Pringle, Martin Rees and Chris Tout for helpful

discussions. The numerical simulations were performed on the COSMOS (SGI Altix 3700) supercomputer at DAMTP in Cambridge and on the Cambridge High Performance Computing Cluster DARWIN in Cambridge. COSMOS is a UK-CCC facility which is supported by HEFCE and PPARC. DARWIN is the primary supercomputer of the University of Cambridge High Performance Computing Service (<http://www.hpc.cam.ac.uk/>), provided by Dell Inc. using Strategic Research Infrastructure Funding from the Higher Education Funding Council for England. Special thanks to Amanda Smith for using her artistic wizardry in preparing Figure 5.

REFERENCES

- Bastian N., Goodwin S. P., 2006, MNRAS, 369, L9
 Begelman M. C., 2001, ApJ, 551, 897
 Begelman M. C., Blandford R. D., Rees M. J., 1984, Reviews of Modern Physics, 56, 255
 Begelman M. C., Rees M. J., 1978, MNRAS, 185, 847
 Begelman M. C., Rossi E. M., Armitage P. J., 2008, MNRAS, 387, 1649
 Begelman M. C., Volonteri M., Rees M. J., 2006, MNRAS, 370, 289
 Belokurov V., Zucker D. B., Evans N. W., Kleya J. T., Koposov S., Hodgkin S. T., Irwin M. J., Gilmore G., Wilkinson M. I., Fellhauer M., Bramich D. M., Hewett P. C., Vidrih S., De Jong J. T. A., Smith J. A., Rix H.-W., Bell E. F., Wyse R. F. G., 2007, ApJ, 654, 897
 Bernadetta D., Volonteri M., 2008, ArXiv e-prints
 Binney J., Tremaine S., 1987, Galactic dynamics. Princeton, NJ, Princeton University Press, 1987, 747 p.
 Blandford R. D., Begelman M. C., 1999, MNRAS, 303, L1
 Böker T., Laine S., van der Marel R. P., Sarzi M., Rix H.-W., Ho L. C., Shields J. C., 2002, AJ, 123, 1389
 Bromm V., Loeb A., 2003, ApJ, 596, 34
 Bryan G. L., Norman M. L., 1995, Bulletin of the American Astronomical Society, 27, 1421
 Bryan G. L., Norman M. L., 1997, in ASP Conf. Ser. 123: Computational Astrophysics; 12th Kingston Meeting on Theoretical Astrophysics Simulating X-Ray Clusters with Adaptive Mesh Refinement. pp 363–+
 Carollo C. M., Stiavelli M., de Zeeuw P. T., Mack J., 1997, AJ, 114, 2366
 Carollo C. M., Stiavelli M., Mack J., 1998, AJ, 116, 68
 Chandrasekhar S., 1964a, Physical Review Letters, 12, 114
 Chandrasekhar S., 1964b, ApJ, 140, 417
 Côté P., Piatek S., Ferrarese L., Jordán A., Merritt D., Peng E. W., Hasegan M., Blakeslee J. P., Mei S., West M. J., Milosavljević M., Tonry J. L., 2006, ApJS, 165, 57
 Dijkstra M., Haiman Z., Mesinger A., Wyithe S., 2008, ArXiv e-prints
 Eisenstein D. J., Loeb A., 1995, ApJ, 443, 11
 Fan X., Carilli C. L., Keating B., 2006, ARA&A, 44, 415
 Fan X. e. a., 2001, AJ, 122, 2833
 Freitag M., 2008, in Beuther H., Linz H., Henning T., eds, Massive Star Formation: Observations Confront Theory Vol. 387 of Astronomical Society of the Pacific Conference Series, Stellar Collisions in Young Clusters: Formation of (Very) Massive Stars?. pp 247–+
 Gammie C. F., 1998, MNRAS, 297, 929

- Glover S. C. O., Brand P. W. J. L., 2001, *MNRAS*, 321, 385
- Greif T. H., Johnson J. L., Klessen R. S., Bromm V., 2008, *ArXiv e-prints*, 803
- Gürkan M. A., Fregeau J. M., Rasio F. A., 2006, *ApJ*, 640, L39
- Haehnelt M. G., Rees M. J., 1993, *MNRAS*, 263, 168
- Haiman Z., 2006, *New Astronomy Review*, 50, 672
- Haiman Z., Loeb A., 2001, *ApJ*, 552, 459
- Hoyle F., Fowler W. A., 1963a, *Nature*, 197, 533
- Hoyle F., Fowler W. A., 1963b, *MNRAS*, 125, 169
- Kauffmann G., Haehnelt M., 2000, *MNRAS*, 311, 576
- Koushiappas S. M., Bullock J. S., Dekel A., 2004, *MNRAS*, 354, 292
- Lin D. N. C., Pringle J. E., 1987, *MNRAS*, 225, 607
- Lin D. N. C., Pringle J. E., 1990, *ApJ*, 358, 515
- Lodato G., Natarajan P., 2006, *MNRAS*, 371, 1813
- Merritt D., 2008, *ArXiv e-prints*, 802
- Mészáros P., Rees M. J., 2001, *ApJ*, 556, L37
- Mo H. J., Mao S., White S. D. M., 1998, *MNRAS*, 295, 319
- Mundt R., Buehrke T., Solf J., Ray T. P., Raga A. C., 1990, *A&A*, 232, 37
- Norman M. L., 2008, in O'Shea B. W., Heger A., eds, *First Stars III Vol. 990 of American Institute of Physics Conference Series, Population III Star Formation and IMF*. pp 3–15
- Norman M. L., Bryan G. L., 1999, in Miyama S. M., Tomisaka K., Hanawa T., eds, *ASSL Vol. 240: Numerical Astrophysics Cosmological Adaptive Mesh Refinement*. pp 19–+
- Oh S. P., Haiman Z., 2002, *ApJ*, 569, 558
- Omukai K., Nishi R., 1999, *ApJ*, 518, 64
- Omukai K., Schneider R., Haiman Z., 2008, *ArXiv e-prints*, 804
- O'Shea B. W., Bryan G., Bordner J., Norman M. L., Abel T., Harkness R., Kritsuk A., 2004, *ArXiv Astrophysics e-prints*
- Portegies Zwart S. F., Baumgardt H., Hut P., Makino J., McMillan S. L. W., 2004, *Nature*, 428, 724
- Rees M. J., 1978, *Phys. Scr*, 17, 193
- Rees M. J., 1984, *ARA&A*, 22, 471
- Regan J. A., Haehnelt M. G., 2008, *ArXiv e-prints*
- Seth A., Agüeros M., Lee D., Basu-Zych A., 2008, *ApJ*, 678, 116
- Shakura N. I., Syunyaev R. A., 1973, *A&A*, 24, 337
- Shapiro S. L., Teukolsky S. A., 1979, *ApJ*, 234, L177
- Shapiro S. L., Teukolsky S. A., 1983, *Black holes, white dwarfs, and neutron stars: The physics of compact objects. Research supported by the National Science Foundation*. New York, Wiley-Interscience, 1983, 663 p.
- Shlosman I., Begelman M. C., Frank J., 1990, *Nature*, 345, 679
- Shlosman I., Frank J., Begelman M. C., 1989, *Nature*, 338, 45
- Spitzer L. J., 1969, *ApJ*, 158, L139+
- Tanaka T., Haiman Z., 2008, *ArXiv e-prints*
- Thorne K. S., Zytkov A. N., 1977, *ApJ*, 212, 832
- Toomre A., 1964, *ApJ*, 139, 1217
- Turner N. J., Blaes O. M., Socrates A., Begelman M. C., Davis S. W., 2005, *ApJ*, 624, 267
- Umemura M., Loeb A., Turner E. L., 1993, *ApJ*, 419, 459
- Volonteri M., 2007, *ArXiv e-prints*, 709
- Volonteri M., Haardt F., Madau P., 2003, *ApJ*, 582, 559
- Volonteri M., Lodato G., Natarajan P., 2008, *MNRAS*, 383, 1079
- Volonteri M., Rees M. J., 2005, *ApJ*, 633, 624
- Whalen D., van Veelen B., O'Shea B. W., Norman M. L., 2008, *ApJ*, 682, 49
- White S. D. M., Rees M. J., 1978, *MNRAS*, 183, 341
- Wise J. H., Turk M. J., Abel T., 2007, *ArXiv e-prints*, 710
- Zel'Dovich Y. B., 1970, *A&A*, 5, 84
- Zel'Dovich Y. B., Novikov I. D., 1967, *Soviet Astronomy*, 10, 602